Nanoscale

PAPER

View Article Online
View Journal

Cite this: DOI: 10.1039/c6nr05014j

Uncovering the density of nanowire surface trap states hidden in the transient photoconductance†

Qiang Xu and Yaping Dan*

Received 22nd June 2016,
Accepted 14th July 2016

DOI: 10.1039/c6nr05014j

www.rsc.org/nanoscale

The gain of nanoscale photoconductors is closely correlated with surface trap states. Mapping out the density of surface trap states in the semiconductor bandgap is crucial for engineering the performance of nanoscale photoconductors. Traditional capacitive techniques for the measurement of surface trap states are not readily applicable to nanoscale devices. Here, we demonstrate a simple technique to extract the information on the density of surface trap states hidden in the transient photoconductance that is widely observed. With this method, we found that the density of surface trap states of a single silicon nanowire is ~10^{12} cm^{-2} eV^{-1} around the middle of the upper half bandgap.

Ultra-scaled one or two dimensional nanostructures may find many important applications in, for instance, flexible electronics[1] and biophotonics.[2] The drawback of nanoscale devices for photo-detection is their weak light absorption due to their ultra-scaled volume,[3,4] which reduces the photosensitivity and signal-to-noise ratio of the devices. High gain is required for high-performance nanoscale photodetectors. Nanosized photoconductors are reported to have extraordinarily high gain (up to 8 orders of magnitude) and have been extensively investigated in the past decade.[3–10] The origin of the high gain is still in dispute but is commonly believed to be correlated with surface trap states.[7,8,11] Mapping out the density and distribution of surface trap states in the semiconductor bandgap[12] is critical for engineering the device performance. However, traditional capacitive techniques for probing the density of surface trap states are not readily applicable to the ultra-scaled nanodevices due to the ubiquitous parasitic capacitances.[13] In this work, we demonstrate a simple but powerful method to uncover the information on the nanowire surface trap states hidden in the transient photoconductance.

Previously we reported that the trap states can be found from the sophisticated frequency dependence of the nanowire photoconductivity.[11] Here, we show a method for extracting the density of trap states in single nanowires from transient photoconductance. The concept is briefly illustrated in Fig. 1. Under small injection conditions, electron–hole pairs (Δn and Δp) will be excited in a highly doped p-type semiconductor, lifting up the electron quasi Fermi level while leaving the hole quasi Fermi level nearly intact. The surface states below the electron quasi Fermi level will be filled with photogenerated electrons (Δn_t), following the Fermi–Dirac distribution. For lightly doped or intrinsic semiconductors, both the electron and hole quasi Fermi levels will shift, allowing photogenerated electrons and holes to be trapped simultaneously. This is a very complicated scenario and will be subjected to further investigation in the future.

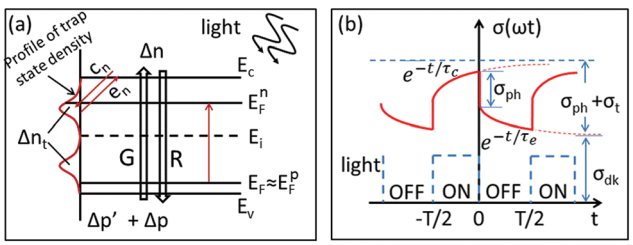

Fig. 1 (a) Generation–recombination (G–R) process from band to band and capture–emission (C–E) process of surface trap states for semiconductors under light illumination. The electron quasi-Fermi level shifts up, allowing for trap states below to be filled up with electrons. The same number of photogenerated holes is left in the valence band for photoconductance. (b) The transient conductance of semiconductors under light illumination. The capture–emission process of surface trap states results in the exponential rise and fall of photoconductance.

The information on the density of surface trap states can be found by differentiating the captured electron concentration Δn_t with respect to the quasi Fermi level shift that is determined by the generation of excess carriers Δn and Δp. Fortunately, Δn_t and the quasi Fermi level can be retrieved separately from the transient photoconductance, since the electron capture by surface states and excess carrier generation in the energy bands, although both contribute to the photo-

University of Michigan–Shanghai Jiao Tong University Joint Institute, Shanghai Jiao Tong University, Shanghai 200240, China. E-mail: yaping.dan@sjtu.edu.cn

†Electronic supplementary information (ESI) available. See DOI: 10.1039/c6nr05014j

conductance directly or indirectly, are two distinct processes in the time domain. More specifically, the generation of excess carriers Δn and Δp is almost immediate upon illumination, while the capture of photogenerated electrons by surface trap states is a slow process that is determined by the capture rate c_n (Fig. 1a). In the time domain, the photoconductance will first immediately jump up and then follow a slow rising process with an exponential characteristic, as shown in the period from $-T/2$ to 0 in Fig. 1b. When the light illumination is cut off, the photoconductance drops suddenly and is then followed by a slow exponential decay. This is because the band-to-band recombination is fast while the trapped electrons emitting back to the conduction band is a slow process.

Based on the analysis above, it is not difficult to write an analytical expression that describes the transient photoconductance as follows:

$$\sigma(t) = \begin{cases} \sigma_d + \sigma_{ph} + \sigma_t - \sigma_t \exp\left(-\dfrac{T}{2\tau_c} + \dfrac{u}{\tau_c}\right)\exp(-t/\tau_c) & -\dfrac{T}{2} < t \le 0 \\ \sigma_d + \sigma_t \exp\left(\dfrac{v}{\tau_e}\right)\exp(-t/\tau_e) & 0 < t \le \dfrac{T}{2} \end{cases} \quad (1)$$

where σ_d is the dark conductance, σ_{ph} the photoconductance coming from Δn and Δp in equilibrium, and σ_t the trap state induced photoconductance contributed by $\Delta p'$ that is the excess holes left in the valence band after the same number of electrons Δn_t are trapped by the surface trap states. T is the chopping period and $\omega = 2\pi/T$. τ_c and τ_e are the capture and emission time constants, respectively. u and v are the constants set to ensure that this equation is continuous with

$$u = \tau_c \ln\left(\frac{1 - \exp\left(\dfrac{T}{2\tau_e}\right)}{\exp\left(-\dfrac{T}{2\tau_c}\right) - \exp\left(\dfrac{T}{2\tau_e}\right)}\right), \quad \text{and}$$

$$v = \tau_e \ln\left(\frac{1 - \exp\left(\dfrac{T}{2\tau_c}\right)}{\exp\left(-\dfrac{T}{2\tau_e}\right) - \exp\left(\dfrac{T}{2\tau_c}\right)}\right).$$

By fitting eqn (1) into experimental data, we could retrieve all the unknown parameters including σ_{ph} and σ_t, from which the electron quasi Fermi level and the number of trapped electrons can also be found for deriving the density of surface trap states. To do so, we isolated single silicon nanowires that were in contact with four microelectrodes (180 nm-thick Al on top of 20 nm-thick Co) on the n^+-Si/SiO_2 substrate (300 nm thick SiO_2) by photolithography and thermal evaporation, as shown in Fig. 2a. The nanowires were synthesized by the Au-catalyzed vapor–liquid–solid (VLS) method, the details of which can be found in our previous publication.[14] The crystal structure of the nanowires was examined using a transmission electron microscope (TEM, Fig. 2b), which showed that the nanowire is single crystalline while the surface is covered with amorphous native oxide (SiO_x). The single crystalline structure makes us believe that the density of trap states extracted from the experimental results below mostly accounted for the trap states on nanowire surfaces.

After the metal contacts were thermally annealed in forming gas at 260 °C for 15 min, the nanowire devices typically show a linear current *vs.* voltage (*I*–*V*) curve (Fig. 2c, recorded using a computer-controlled Keithley sourcemeter

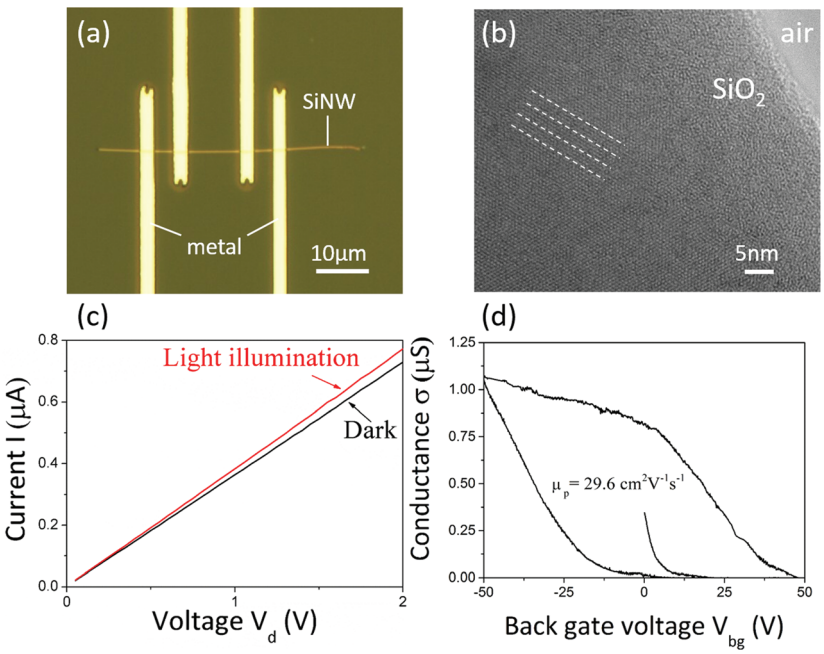

Fig. 2 (a) Optical microscope image of a silicon nanowire in contact with four microelectrodes. (b) TEM image showing that the SiNW is single crystalline while the surface is covered with amorphous native oxide (SiO_x). (c) Current *vs.* voltage (*I*–*V*) curve for a nanowire with or without light illumination. (d) Transfer characteristics for a SiNW FET with a source–drain bias of V_{ds} = 0.02 V. Back gate voltage V_{bg} is applied to the substrate.

2400) and is responsive to light illumination. The linear IV characteristics indicate that the contacts between the nanowire and contact electrodes are ohmic. The extracted contact resistances are negligibly small compared to the nanowire resistance. To find the charge carrier mobility in the nanowire, we investigated the transfer characteristics using the highly doped substrate as the back gate. The transconductance exhibits a large hysteresis loop (Fig. 2d) due to the trap states in the nanowires. The size of the loop depends on the range of sweeping gate voltage (see Fig. S1 in the ESI†). Although the hysteresis loop has been used to estimate the trap states in the thin film devices,[15] the method would be inaccurate when applied to the nanowire on the Si/SiO_2 substrate since the band bending on the cylindrical nanowire surfaces is uneven. When the device is turned on, the transconductance σ_{ds} is linearly dependent on the gate voltage V_{bg} on both sides of the loop. By averaging the slope of both sides, the hole mobility can be estimated to be 29.6 $cm^2\ V^{-1}\ s^{-1}$ from the expression $\mu_p = (d\sigma_{ds}/dV_{bg}) \times (L^2/C)$,[16] where L is the nanowire device length (7.1 μm) and C is the capacitance between the nanowire device and the n^+-Si substrate. The capacitance C is given by $C \approx 2\pi\varepsilon\varepsilon_0 L/\ln(2h/r)$ using the cylinder-on-plate model,[16] where ε is the SiO_2 relative dielectric constant (3.9), h the thickness of the silicon oxide layer (= 300 nm), and r the SiNW radius (26.5 nm, examined by the scanning electron microscope (SEM) image in ESI Fig. S2†). Given the hole mobility, we found that the boron doping concentration in the nanowire is 2.48×10^{18} cm^{-3} from the conductivity given by four probe measurements (see eqn (S1) in the ESI†).

As shown in Fig. 2c, the nanowire devices are responsive to the illumination of a diode-pumped solid-state (DPSS) laser (λ = 532 nm, CNI Lasers) that is coupled to the nanowire through an optical fiber. The diagram of the experimental setup is shown in ESI Fig. S3.† When the light illumination is switched ON/OFF periodically, the nanowire photoconductance follows a pattern similar to the theoretical curve in Fig. 1b, as shown in Fig. 3a. We choose one period of the transient photoconductance and shift it in the time domain to ensure that the curve is centered at $t = 0$ (Fig. 3b). The fittings indicate that the transient photoconductance follows the function below:

$$\sigma(t) = \begin{cases} 3.95 \times 10^{-7} - 2.3 \times 10^{-11} e^{-t/5.2} & -\dfrac{T}{2} < t \le 0 \\ 3.69 \times 10^{-7} + 1.0 \times 10^{-8} e^{-t/14.2} & 0 < t \le \dfrac{T}{2} \end{cases} \quad (2)$$

It is not hard to find that σ_{ph} = 16 nS, σ_t = 10 nS, τ_c = 5.2 s and τ_e = 14.2 s by comparing eqn (2) with eqn (1). The noise is relatively large from one cycle to another (Fig. 3a) since the experiments are performed in an ambient environment. To reduce the noise, we repeat the fitting up to 9 periods of experimental data and statistically find that σ_{ph} = 15.8 ± 0.4 nS, σ_t = 9.7 ± 0.9 nS under illumination of the light intensity of 28 W cm^{-2}. Note that in our experiments, the light is coupled from a solid-state laser to a fiber that guides the light to illuminate the device. The light intensity is our rough estimate and is only accurate in relative terms. Although inaccurate in absolute terms, it does not affect the accuracy for finding the density of nanowire surface trap states as shown later.

We linearly tuned the light intensity and repeated the fittings for all cycles in the same way as described above. The detailed results can be found in ESI Fig. S4–S14.† From σ_{ph}, we find Δn and $\Delta p (= \Delta n)$ following the equation below:

$$\sigma_{ph} = (e\mu_n \Delta n + e\mu_p \Delta p)\frac{A_c}{L} \quad (3)$$

where e, μ_n, μ_p, A_c and L are the unit charge, electron and hole mobility, nanowire cross-section area and length, respectively. Given the low-field hole mobility of 29.6 $cm^2\ V^{-1}\ s^{-1}$, the electron mobility can be roughly estimated to be ~90 $cm^2\ V^{-1}\ s^{-1}$. From eqn (3), we find Δn and then the electron quasi Fermi level (Fig. 4a) for the silicon nanowire device under investigation, which is 53 nm in diameter (Fig. S2 in the ESI†) and 7.1 μm long between the two inner-electrodes. The photoconductance is approximately linear with the light intensity, indicating that the small injection condition is always main-

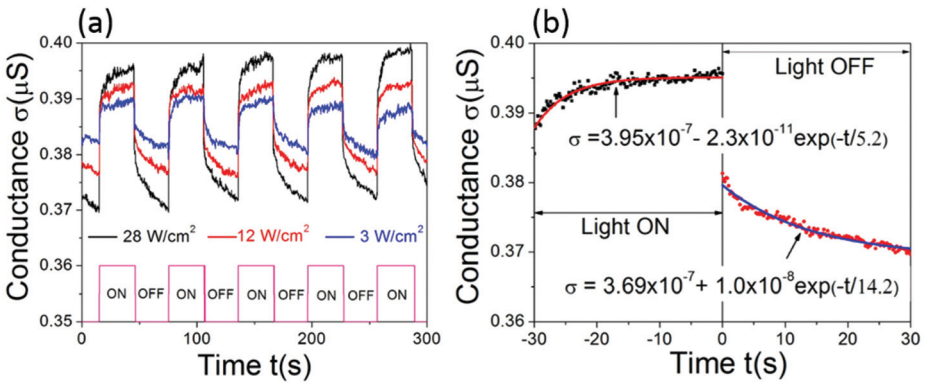

Fig. 3 (a) Transient conductance when the light illumination is switched ON/OFF periodically. (b) Experimental data fitting for one period.

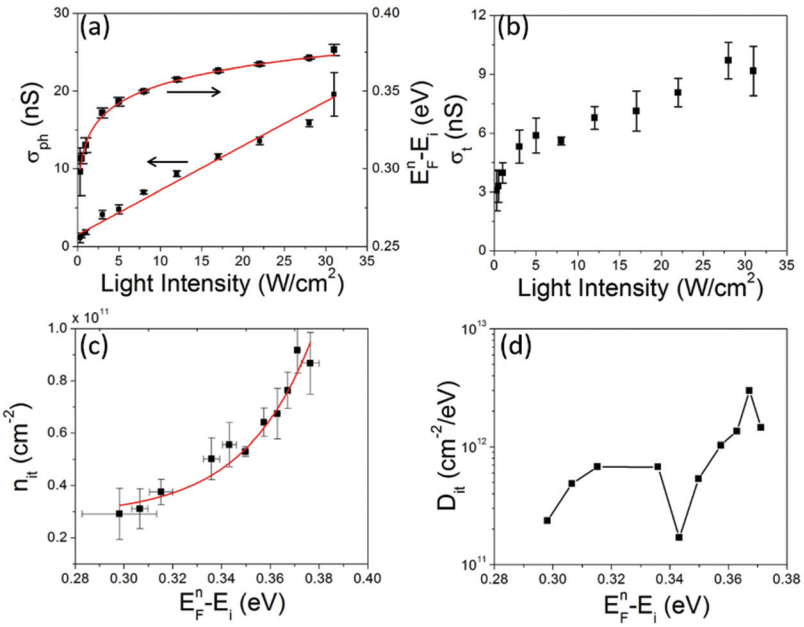

Fig. 4 (a) Photoconductance and electron quasi-Fermi level shift as a function of light intensity. (b) Trap-induced photoconductance as a function of light intensity. (c) Surface concentration of electrons captured by the trap states below the quasi-Fermi level. The red line is given to guide the eye. (d) Density of surface trap states calculated from the data in (c).

tained. It is known that the electron quasi Fermi level $E_F{}^n$ is logarithmically dependent on the photogenerated excess electrons Δn in the conduction band. It is therefore not surprising that $E_F{}^n$ follows a logarithmic function of light intensity (Fig. 4a). The photoconductance σ_t induced by the surface trap states is plotted in Fig. 4b. Since the small injection condition is always maintained, only electrons are involved in the trapping process. The hole counterpart remaining in the valence band contributes to the photoconductance σ_t, that is:

$$\sigma_t = e\mu_p \Delta p' \frac{A_c}{L} \quad (4)$$

From the above equation, we found the concentration of holes $\Delta p'$ in the valence band after the same amount of electrons were captured by the surface trap states.

Fig. 4c shows the correlation of the trapped electron surface concentration with the location of the electron quasi Fermi level. The trapped electron concentration rapidly increases as the quasi Fermi level moves up, indicating more states were filled with electrons. This is consistent with the physics picture described at the beginning of this Letter. We found the density of surface trap states by simply differentiating the surface concentration of trapped electrons with respect to the quasi Fermi level, as shown in Fig. 4d. The trend of the trap state density is in line with what we previously obtained in a different approach.[11,12] Unfortunately, the density obtained here is located in a relatively narrow range near the middle of the upper half bandgap. The higher end of the range is capped by the maximum light intensity illuminated on the nanowire. A higher laser power and better laser-to-fiber coupling efficiency will increase the light intensity, shifting the electron quasi Fermi level closer to the conduction band. The lower end is limited by the relatively noisy low-frequency signals. Since the flicker noise rapidly decreases at high frequencies, the noise will be lower for devices with short capture and emission time constants. In this case the Fermi level can be potentially extended closer to the middle bandgap, allowing this technique to probe trap states in a wide range of distributions. The capture of photogenerated charge carriers by surface trap states will inevitably change the net surface charges and induce energy band bending, acting like a gate for the nanowire device. This gating effect is widely employed to explain the photoconductance gain in nanoscale photoconductors.[6,17,18] However, the gating effect is not an independent effect. It is instead strongly dependent on the density of surface trap states and other surface properties such as initial net surface charges. The transient behavior (rise and fall times) induced by the gating effect is essentially determined by capture and emission lifetimes of trap states. It is more appropriate to incorporate the gating effect into our model presented in this article. The density of surface trap states extracted from the transient photoconductance includes the gating effect if it exists.

In conclusion, we demonstrated a simple but powerful method to uncover the density of surface trap states hidden in the transient photoconductance. In terms of accuracy, the method outperforms the traditional capacitance–voltage (*CV*) method, although the data presented in this Letter is relatively noisy, which is likely due to the nature of the low-frequency signals involved. The performance of nanoscale photo-

conductors is directly correlated with the density of surface trap states. This work opens up a new route for designing photoconductors by engineering the device surfaces.

Acknowledgements

The work was supported by the national "1000 Young Scholars" programme of the Chinese central government, the National Science Foundation of China (61376001) and the SJTU-UM Collaborative Research Program.

References

1 M. C. McAlpine, H. Ahmad, D. W. Wang and J. R. Heath, Highly ordered nanowire arrays on plastic substrates for ultrasensitive flexible chemical sensors, *Nat. Mater.*, 2007, **6**(5), 379–384.
2 R. X. Yan, J. H. Park, Y. Choi, C. J. Heo, S. M. Yang, L. P. Lee and P. D. Yang, Nanowire-based single-cell endoscopy, *Nat. Nanotechnol.*, 2012, **7**(3), 191–196.
3 L. Tang, S. E. Kocabas, S. Latif, A. K. Okyay, D.-S. Ly-Gagnon, K. C. Saraswat and D. A. B. Miller, Nanometre-scale germanium photodetector enhanced by a near-infrared dipole antenna, *Nat. Photonics*, 2008, **2**(4), 226–229.
4 G. K. Felic, F. Al-Dirini, F. M. Hossain, T. N. Cong and E. Skafidas, Silicon nanowire photodetector enhanced by a bow-tie antenna, *Appl. Phys. A: Mater. Sci. Process.*, 2014, **115**(2), 491–493.
5 A. d. L. Bugallo, M. Tchernycheva, G. Jacopin, L. Rigutti, F. H. Julien, S.-T. Chou, Y.-T. Lin, P.-H. Tseng and L.-W. Tu, Visible-blind photodetector based on p-i-n junction GaN nanowire ensembles, *Nanotechnology*, 2010, **21**, 315201.
6 C. Soci, A. Zhang, X. Y. Bao, H. Kim, Y. Lo and D. L. Wang, Nanowire Photodetectors, *J. Nanosci. Nanotechnol.*, 2010, **10**(3), 1430–1449.
7 A. Zhang, H. Kim, J. Cheng and Y. H. Lo, Ultrahigh Responsivity Visible and Infrared Detection Using Silicon Nanowire Phototransistors, *Nano Lett.*, 2010, **10**(6), 2117–2120.
8 S. Lee, S. W. Jung, S. Park, J. Ahn, S. J. Hong, H. J. Yoo, M. H. Lee and D. I. Cho, IEEE in Ultra-high responsivity, silicon nanowire photodetectors for retinal prosthesis, *25th IEEE International Conference on Micro Electro Mechanical Systems (MEMS), Paris, France, Jan 29–Feb 02*; IEEE, Paris, France, 2012.
9 Z. X. Wang, M. Safdar, C. Jiang and J. He, High-Performance UV-Visible-NIR Broad Spectral Photodetectors Based on One-Dimensional In2Te3 Nanostructures, *Nano Lett.*, 2012, **12**(9), 4715–4721.
10 H. Park and K. B. Crozier, Vertically Stacked Photodetector Devices Containing Silicon Nanowires with Engineered Absorption Spectra, *ACS Photonics*, 2015, **2**(4), 544–549.
11 Y. Dan, Optoelectronically probing the density of nanowire surface trap states to the single state limit, *Appl. Phys. Lett.*, 2015, **106**, 053117.
12 E. C. Garnett, Y. C. Tseng, D. R. Khanal, J. Q. Wu, J. Bokor and P. D. Yang, Dopant profiling and surface analysis of silicon nanowires using capacitance-voltage measurements, *Nat. Nanotechnol.*, 2009, **4**(5), 311–314.
13 J. Wu, A. S. Babadi, D. Jacobsson, J. Colvin, S. Yngman, R. Timm, E. Lind and L.-E. Wemersson, Low Trap Density in InAs/High-k Nanowire Gate Stacks with Optimized Growth and Doping Conditions, *Nano Lett.*, 2016, **16**(4), 2418–2425.
14 Y. Dan, K. Seo, K. Takei, J. H. Meza, A. Javey and K. B. Crozier, Dramatic Reduction of Surface Recombination by in Situ Surface Passivation of Silicon Nanowires, *Nano Lett.*, 2011, **11**(6), 2527–2532.
15 H.-C. Lin, C.-H. Hung, W.-C. Chen, Z.-M. Lin, H.-H. Hsu and T.-Y. Hunag, Origin of hysteresis in current–voltage characteristics of polycrystalline silicon thin-film transistors, *J. Appl. Phys.*, 2009, **105**, 054502.
16 Y. Cui, X. F. Duan, J. T. Hu and C. M. Lieber, Doping and electrical transport in silicon nanowires, *J. Phys. Chem. B*, 2000, **104**(22), 5213–5216.
17 C. Soci, A. Zhang, B. Xiang, S. A. Dayeh, D. P. R. Aplin, J. Park, X. Y. Bao, Y. H. Lo and D. Wang, ZnO nanowire UV photodetectors with high internal gain, *Nano Lett.*, 2007, **7**(4), 1003–1009.
18 C.-J. Kim, H.-S. Lee, Y.-J. Cho, K. Kang and M.-H. Jo, Diameter-Dependent Internal Gain in Ohmic Ge Nanowire Photodetectors, *Nano Lett.*, 2010, **10**(6), 2043–2048.